DOI: 10.1039/c5fd00091b

Faraday Discussions

Cite this: *Faraday Discuss.*, 2015, **183**, 389

PAPER

CO_2 capture and electrochemical conversion using superbasic $[P_{66614}]$-[124Triz]

Nathan Hollingsworth,*[a] S. F. Rebecca Taylor,*[b] Miguel T. Galante,[c] Johan Jacquemin,[b] Claudia Longo,[c] Katherine B. Holt,[a] Nora H. de Leeuw[ad] and Christopher Hardacre*[b]

Received 22nd May 2015, Accepted 3rd July 2015
DOI: 10.1039/c5fd00091b

The ionic liquid trihexyltetradecylphosphonium 1,2,4-triazolide, $[P_{66614}][124Triz]$, has been shown to chemisorb CO_2 through equimolar binding of the carbon dioxide with the 1,2,4-triazolide anion. This leads to a possible new, low energy pathway for the electrochemical reduction of carbon dioxide to formate and syngas at low overpotentials, utilizing this reactive ionic liquid media. Herein, an electrochemical investigation of water and carbon dioxide addition to the $[P_{66614}][124Triz]$ on gold and platinum working electrodes is reported. Electrolysis measurements have been performed using CO_2 saturated $[P_{66614}][124Triz]$ based solutions at −0.9 V and −1.9 V on gold and platinum electrodes. The effects of the electrode material on the formation of formate and syngas using these solutions are presented and discussed.

1 Introduction

Since the industrial revolution, the harnessing of fossil fuels by combustion for energy and transportation has seen levels of CO_2 in the atmosphere steadily rise.[1,2] One concern is the increasing concentration of CO_2 in the atmosphere is connected with rising global temperatures and sea levels.[3] Given the potential implications of global warming, strategies to capture and/or convert CO_2 provide the subject of much scientific endeavour.[4]

Aside from a greenhouse gas, CO_2 can be considered as an abundant, renewable and low cost C1 building block for the production of fuels, or as a feedstock for industrial chemical synthesis. The synthesis of fuels is particularly attractive given the carbon neutrality of the product.

[a]*Department of Chemistry, University College London, 20 Gordon Street, London, WC1H 0AJ, UK. E-mail: n.hollingsworth@ucl.ac.uk*
[b]*School of Chemistry and Chemical Engineering, Queen's University Belfast, Belfast, N. Ireland, BT9 5AG, UK. E-mail: r.taylor@qub.ac.uk; c.hardacre@qub.ac.uk*
[c]*Institute of Chemistry, University of Campinas – UNICAMP, Campinas, SP, Brazil*
[d]*School of Chemistry, Cardiff University, Cardiff, CF10 3XQ, UK*

Electrochemical reduction offers a viable route to this goal due to the potential to reduce CO_2 at high efficiencies and selectivity, as well as the ability to harness electrical energy from renewable sources.[5,6] The main barriers are the thermodynamic stability and the kinetic inertness of CO_2, due to the fact that the first electron reduction of linear CO_2 to form the bent $[^{\bullet}CO_2]^-$ radical anion requires a high reduction potential, -1.9 V *vs.* NHE.[7] Attempts have been made to reduce this potential by employing various catalysts, such as the recently reported reductions on Fe_3S_4 surfaces.[8]

Ionic liquids (ILs) have been employed as CO_2 capture agents and electrochemical conversion media due to their intrinsic ionic conductivity, wide potential windows and CO_2 solubility levels.[9–12] ILs generally physically absorb CO_2 into the solution free volume. Reports have shown that ILs can act to stabilise the first electron reduction of the physically absorbed CO_2 by complexation of the reduction product with the IL cation.[12] This significantly reduces the energy required to form the $[^{\bullet}CO_2]^-$ radical anion. Initial CO_2 electrochemical reduction experiments in ILs employed 1-alkyl-3-methylimidazolium ($[C_n\text{mim}]^+$) based ILs with a range of non-coordinating anions such as $[BF_4]^-$, Br^-, Cl^-. The electrochemically generated anion radical, $[^{\bullet}CO_2]^-$, was then reacted with alcohols forming dialkyl carbonates.[13–15]

Further studies used hydrated ILs, to provide a source of H^+. CO_2 physically absorbed within the IL was reduced with Ag, as the working electrode, further enabling the reduction of the IL stabilised $[^{\bullet}CO_2]^-$ to CO, as shown in the Scheme 1.[12]

CO_2 reduced to CO in a hydrated IL $[C_2\text{mim}][BF_4]$ on a Ag working electrode was reported to have overpotentials as low as 0.2 V.[12] H_2 production was also suppressed due to the cation forming a monolayer on the electrode surface.[16] Further improvements have been reported by employing a MoS_2 working electrode, resulting in overpotentials as low as 0.054 V.[17]

Product selectivity has also been observed upon altering the IL anion. For example, using $[C_2\text{mim}]^+$ based ILs on Pb electrodes, oxalate is favoured in the presence of $[NTf_2]^-$ and formate is favoured when $[TFA]^-$ is used.[9,11]

Recently, we have reported an alternative route for CO_2 reduction in ILs, by using $[P_{66614}][124\text{Triz}]$.[18] $[P_{66614}][124\text{Triz}]$ is able to capture significantly more CO_2 than ILs such as $[C_4\text{mim}][NTf_2]$ or $[C_2\text{mim}][OAc]$, due to the chemical reactivity of the 1,2,4-triazolide anion.[19] The anion can chemically bind CO_2 allowing up to equimolar amounts of CO_2 to be captured, as illustrated in the Scheme 2.[19]

Crucially, upon binding, the CO_2 geometry is altered from linear to bent. A lower energy pathway to CO_2 reduction was demonstrated in this IL, which may be related to the chemical binding of the CO_2 by the anion.[18] $[P_{66614}][124\text{Triz}]$ is also able to absorb CO_2 through physical exothermic absorption in the solution free

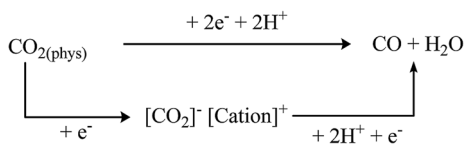

Scheme 1 Reduction of CO_2 to CO in an IL, which absorbs CO_2 physically.[12]

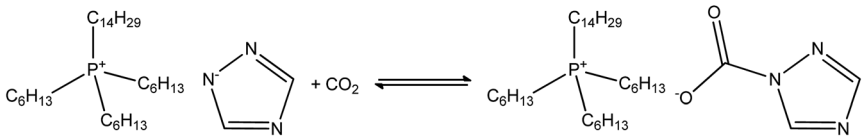

Scheme 2 CO_2 binding to the $[124Triz]^-$ anion in the IL $[P_{66614}][124Triz]$.[19]

volume that is driven by an entropic process of solvation. The physically absorbed CO_2 may also undergo reduction stabilised by the $[P_{66614}]^+$ cation. Formate was produced by the lower energy route at −0.7 V *vs.* $Ag/AgNO_3$ with 95% Faradaic efficiency on the Ag electrodes. In addition, reduction of the physically absorbed CO_2 at −1.9 V *vs.* $Ag/AgNO_3$ produced CO with a 41% Faradaic efficiency.[18] In comparison, on using $[P_{66614}][NTf_2]$ or $[P_{66614}][BF_4]$, which do not support chemical CO_2 binding, little or no product was formed at −0.7 V suggesting that the reaction occurring at less negative potentials (*i.e.* −0.7 V) in $[P_{66614}][124Triz]$ is related to the reduction of chemically bound CO_2 (Scheme 2). Products were formed at −1.9 V, *i.e.* the same potential as found in $[P_{66614}][124Triz]$, indicating that they are formed from the reduction of physically absorbed CO_2 stabilised by the $[P_{66614}]^+$ cation (Scheme 1).[18] Herein, the study is expanded to investigate the influence of the electrode material on the CO_2 reduction potential, product distribution and Faradaic efficiency.

2 Experimental

2.1 Materials and IL synthesis

Trihexyltetradecylphosphonium chloride ($[P_{66614}]Cl$) was received from Cytec (97.7%) and 1,2,4-triazole (98%) was purchased from Sigma-Aldrich. The Au foil (0.1 mm thick 99.9975+%) and Pt wire (0.3 mm dia., 99.99%) were purchased from Alfa Aesar. Gaseous nitrogen (99.998%) and carbon dioxide (99.99%) were obtained from BOC and passed through drying columns before contact with the IL samples. The water was purified using a Milli-Q 18.3 MΩ water system.

$[P_{66614}][124Triz]$ was prepared using a previously reported method[20] and a two step synthesis procedure; $[P_{66614}][OH]$ was synthesized using an anion exchange resin from $[P_{66614}]Cl$ followed by addition of the superbase. The water content of the ILs was measured using a Metrohm 787 KF Titrino Karl Fischer and was found to be <0.1 wt% for all ILs. Halide content was below the detectable limit by testing with $AgNO_3$.

2.2 Electrochemical experiments

Cyclic voltammograms (CVs) were recorded using an Ecochemie Autolab Potentiostat/Galvanostat (PGSTAT302) and carried out using a three-electrode arrangement with a Au or Pt working electrode (1.6 mm), a platinum coil as the counter electrode. All potentials were measured with respect to a 0.01 mol L^{-1} Ag/Ag^+ reference, with $AgNO_3$ dissolved in $[C_4mim][NO_3]$ and separated from the bulk solution *via* a glass frit. Electrolysis experiments were carried out using a three electrode set up in a sealed 50 cm^3 cell with a gas tight syringe attached. The working electrodes were a coiled Pt wire or a Au foil, a Pt coil was used as the

counter electrode (contained within a counter compartment) and the potentials were measured with respect to a 0.01 mol L^{-1} Ag/Ag^+ reference, with $AgNO_3$ dissolved in $[C_4mim][NO_3]$ and separated from the bulk solution *via* a glass frit. A 0.1 mol L^{-1} $[P_{66614}][124Triz]$, 0.7 mol L^{-1} H_2O in acetonitrile solution (8 cm^3) was added to the cell and bubbled with CO_2 (25 cm^3 min^{-1}) for 60 min, during this time the gas syringe was gradually opened. The cell was then sealed, connected up to a potentiostat (Biologic VMP3 controlled by EC-Lab) and a potential applied to the cell for the time required to pass 10 C of charge. It should be noted that no ionic liquid decomposition or reaction was observed under any of the conditions tested in this study.

2.3 Solution phase detection

Solution samples were analysed by obtaining ^1H NMR spectra using a Bruker Avance III 600 with a DCH cryoprobe. Quantitative analysis was performed using the ERETIC2 quantification tool within Topspin 3.2.

2.4 Gas phase detection

The gas phase of the reaction was analysed using a Perkin-Elmer Clarus 500 Gas Chromatograph equipped with a TCD and FID (with methanizer) fitted with a packed column (stainless steel, 30 ft, 1/8 inch OD, 2.0 mm ID packed with Haysep DB 100/120 mesh). The gaseous products were transferred to the GC by connecting up the cell and injecting the contents of the gas tight syringe attached to the cell into the GC. H_2 was quantified using the TCD and CO using the FID.

3 Results and discussion

3.1 Voltammetry study of CO_2 reduction in $[P_{66614}][124Triz]$ using various working electrodes

CVs have been recorded at both Au and Pt electrodes in 0.1 mol L^{-1} $[P_{66614}]$-$[124Triz]$ in acetonitrile (MeCN). CVs were recorded at a scan rate of 100 mV s^{-1} at 22 °C. The reference electrode was a previously reported 0.01 mol L^{-1} Ag/Ag^+ reference, with $AgNO_3$ dissolved in $[C_4mim][NO_3]$ and separated from the bulk solution *via* a glass frit.[21,22] 0.1 mol L^{-1} $[P_{66614}][124Triz]$ in MeCN was first saturated with argon and a baseline CV taken. Thereafter, water was added (0.7 mol L^{-1}), as a source of H^+ and the influence on the CV investigated. The H^+ is required to make protonated reduction products and CO through the reaction of reduced CO_2 and H^+ (Scheme 1). Finally, the hydrated IL mixture was purged with CO_2 for 30 min and a CV taken to assess CO_2 reduction processes.

3.1.1 Au working electrode. CVs relating to the use of a polished Au working electrode (0.16 cm^2) are displayed in Fig. 1. The CV, after purging with Ar, is shown in blue. A small increase in reduction current is observed at *ca.* −1.1 V with a rapid increase in reduction current at *ca.* −2.0 V. Upon the addition of H_2O to the IL/MeCN mixture, a small increase in current is observed at −1.0 V and a larger increase at *ca.* −1.75 V (Fig. 1, red). Although the small increase in current observed at −1.0 V has a slight anodic shift compared with that observed in the Ar saturated sample (−1.1 V), this feature may be attributed to the reduction of 1,2,4-triazole formed from the reaction of the $[124Triz]^-$ anion and H_2O (Scheme 3).

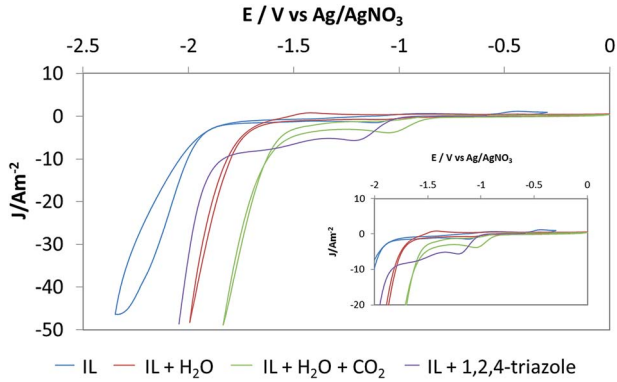

Fig. 1 Cyclic voltammograms of 0.1 mol L^{-1} $[P_{66614}][124Triz]$ (IL) in acetonitrile (MeCN) at a gold electrode; (blue) IL in MeCN; (red) IL in MeCN + 0.7 mol L^{-1} H_2O; and (green) IL in MeCN + 0.7 mol L^{-1} H_2O + CO_2, IL in MeCN + 0.5 mol L^{-1} 1,2,4-trizole; only the cathodic linear sweep is shown for clarity. Magnification is shown inset.

To test this theory, 1,2,4-triazole was deliberately added to a solution of hydrated 0.1 mol L^{-1} $[P_{66614}][124Triz]$ in MeCN. The CV showed that, upon addition of 1,2,4-triazole, the current from −1.0 V increased, supporting this proposal. The presence of the small current increase at −1.1 V in the Ar saturated sample could, therefore, either be due to adventitious water or trace 1,2,4-triazole impurities from the synthesis process of $[P_{66614}][124Triz]$, which is synthesised from the addition of 1,2,4-triazole to $[P_{66614}][OH]$.

The large reduction current at −1.8 V, observed upon the addition of H_2O, shows a large anodic shift compared to the onset of the large reduction current in the Ar saturated sample. This is proposed to be due to the reduction of H_2O to H_2. This region also increases in current when 1,2,4-triazole is deliberately added to the electrolyte, suggesting that generation of H_2 from the reduction of 1,2,4-triazole may also contribute to this current. In addition, a small oxidative stripping peak is observed at −1.5 V, following the rapid increase of current at −1.8 V, suggesting that the product of the reduction may interact with the electrode surface. Recent reports employing $[C_4mim][BF_4]$ on Au surfaces have shown the hydrogen evolution reaction to occur at *ca.* −2.0 V *vs.* Ag/Ag^+,[23] suggesting that the use of chemically co-ordinating IL provides a pathway to less negative reduction potentials.

Saturation of the hydrated IL mixture with CO_2 (Fig. 1 green) resulted in an increase in current at −0.9 V, followed by a rapid increase in current at −1.6 V. The peak at −0.9 V shows an increased current and greater anodic shift when compared to the hydrated sample. The large increase in current observed at −1.6 V shows an anodic shift in comparison to Ar saturated and hydrated samples. Previous reports on Ag electrodes have suggested that the reduction at less negative potentials (−0.7 V) could be assigned to the reduction of CO_2

$$[124Triz]^- + H_2O \longrightarrow [124Triz\text{-}H] + OH^- \quad \ldots(1)$$

Scheme 3 H_2O reaction with the $[124Triz]^-$ anion in the $[P_{66614}][124Triz]$.

chemically bound to the $[124Triz]^-$ anion, while reductions at more negative potentials (−1.9 V) could be assigned to the reduction of physically absorbed CO_2 (Scheme 4 eqn (2)–(5), respectively).[18] The reduction of physically absorbed CO_2 at −1.6 V is in good agreement with CO_2 reduction reported on Au electrodes in $[C_4mim][BF_4]$. Reduction of CO_2 in $[C_4mim][BF_4]$, an IL that only exhibits physical CO_2 absorption, on the Au surface was reported at −1.8 V *vs.* NHE (*i.e.* −1.6 V *vs.* Ag/Ag^+).[23] Interestingly, the potential for the reduction of CO_2 over Au reported, herein, at −0.9 V is the lowest potential, to the best of our knowledge, reported to date using ionic liquid systems showing the potential of reactive IL to enhance the electrochemical activity.

Assuming similar mechanisms take place at the Au electrode, this suggests that chemically bound CO_2 can be reduced at less negative potentials on Ag than Au (−0.7 V compared to −0.9 V), but that the reduction of physically bound CO_2 occurs at less negative potentials on Au than Ag (−1.6 V *vs.* −1.9 V). One plausible explanation would be that Ag is more catalytically active than Au and, therefore, the IL is more strongly bound to the Ag electrode than the Au. This may suggest that the chemically bound CO_2 on Ag can be reduced at less negative potentials due to the increased contact with the electrode but the physically absorbed CO_2 is blocked by the IL requiring more negative potentials for reduction. Reduced binding in the Au system suggests the physically absorbed CO_2 has easier access to the electrode and, therefore, physically absorbed reduction occurs at a less negative potential than on Ag, but that the reduction of the chemically absorbed CO_2 requires a more negative potential than in the Ag system.

3.1.2 Pt working electrode. CVs relating to the use of a polished Pt working electrode (0.16 cm^2) are displayed in Fig. 2, the CV after purging with Ar is shown in blue. An increase in current is observed at −1.6 V followed by the start of a rapid current increase at *ca.* −2.1 V. Upon the addition of H_2O to the IL/MeCN mixture (Fig. 2 red), a rapid increase in current is observed at −1.5 V with no smaller current increase observed at lower potentials. The rapid increase in current at −1.5 V shows an anodic shift and enhanced current compared to the Ar saturated sample. This peak is plausibly associated with the reduction of H_2O to H_2. On comparison with the Au electrode the reduction of H_2O to H_2 takes place at a less negative potential on Pt than Au (−1.5 V *vs.* −1.8 V). This is consistent with Pt being well known as an excellent catalyst for water splitting.

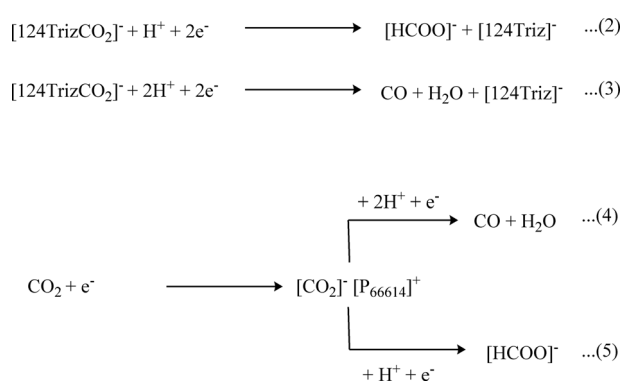

Scheme 4 Suggested CO_2 reduction processes occurring on the working electrode.

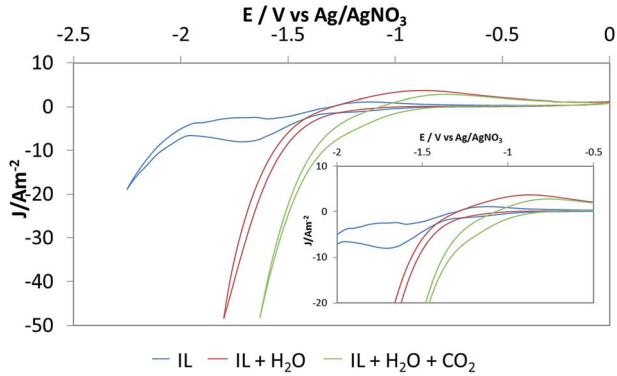

Fig. 2 Cyclic voltammograms of 0.1 mol L^{-1} $[P_{66614}][124Triz]$ (IL) in acetonitrile (MeCN) at a platinum electrode; (blue) IL in MeCN, (red) IL in MeCN + 0.7 mol L^{-1} H_2O, and (green) IL in MeCN + 0.7 mol L^{-1} H_2O + CO_2. Magnified CVs are inset.

Saturating the hydrated IL mixture with CO_2 (Fig. 2 green) results in a slow increase in current at −0.9 V. The increase becomes rapid at −1.4 V. The slow increase in current is plausibly due to the reduction of CO_2 bound to the $[124Triz]^-$ anion, while the rapid increase in current is associated with the reduction of physically absorbed CO_2.

Both Au and Pt display similar reduction potentials for CO_2 bound to the $[124Triz]^-$ anion (−0.9 V), which are more negative than reduction on Ag (−0.7 V). However, the reduction of physically bound CO_2 is less negative for Pt than Au (−1.4 V and −1.6 V respectively), both of which are less negative than Ag (−1.9 V). It is important to note that the Pt is more catalytically active than both the Au and Ag and, therefore, should show a higher activity. However, as a result of this increased activity Pt will also bind the IL more strongly than the Ag, therefore, the results suggest that a balance between activity and adsorption strength is required for CO_2 reduction at lower potentials. As CO is also formed during these experiments and the binding of CO to Pt will be much stronger than on Ag or Au, site blocking from the CO may also be contributing to the observed differences between the electrode performance.

3.2 Electrolysis study

Electrolysis was performed in CO_2 saturated and hydrated (0.7 mol L^{-1} H_2O) 0.1 mol L^{-1} $[P_{66614}][124Triz]$ in MeCN (8 cm^3). Electrolysis was continued until a fixed charge of 10 C had passed, after which the solution phase was tested by quantitative ^1H NMR and in the gas phase by gas chromatography (GC). The reported values for the analogous electrolysis using Ag electrodes is displayed in Fig. 3. While Ag electrodes are reported to display Faradic efficiencies of 95% at −0.7 V, with an applied potential of 0.17 V, electrolysis on Au and Pt at this potential resulted in no detected reduction product. Therefore, electrolysis was also performed at −1.9 V and −0.9 V to test for reduction of physical and chemical absorbed CO_2, respectively, using these electrodes. The experiments were also performed at these potentials with Ag for comparison (Fig. 3 and 4), although it should be noted that electrolysis at −0.9 V is not the optimum potential for formate production on Ag.[18]

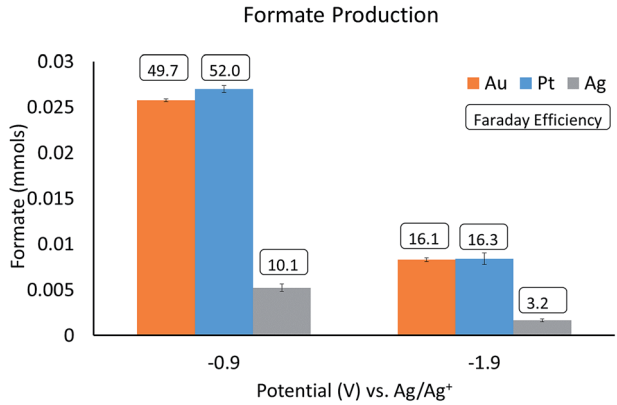

Fig. 3 Quantitative ^{1}H NMR analysis of formate production at the Au, Pt, and Ag electrodes after 10 C of charge is passed. Error bars represent ±1.5 standard deviations. Faraday efficiencies for each potential and electrode are shown in the boxes.

3.2.1 Au electrode. 0.5 cm^2 of Au foil was employed as a working electrode. Quantitative ^{1}H NMR of the electrolyte after electrolysis showed the presence of formate for both investigated potentials (−0.9 V and −1.9 V). The formate produced at −0.9 V is proposed to be formed from the reduction of CO_2 bound to the $[124Triz]^-$ anion (Scheme 4 eqn (2)), while the formate produced at −1.9 V is proposed to be generated from the reduction of physically absorbed CO_2 stabilised by $[P_{66614}]^+$ cation (Scheme 4 eqn (5)). A greater quantity of formate was detected at −0.9 V (0.026 mmol) compared with −1.9 V (0.0083 mmol) with Faradaic efficiencies of 49.7 and 16.1%, respectively. This is in contrast to previous reports using $[C_2mim][TFA]$, whereby the Faradaic efficiency for formate production increases with potential.[9] The open circuit potential (OCP) prior to electrolysis, but after CO_2 saturation, was measured at −0.45 V, suggesting an applied potential of −0.45 and −1.45 V for potential holds of −0.9 and −1.9 V, respectively. A comparison with the reported values for the analogous electrolysis

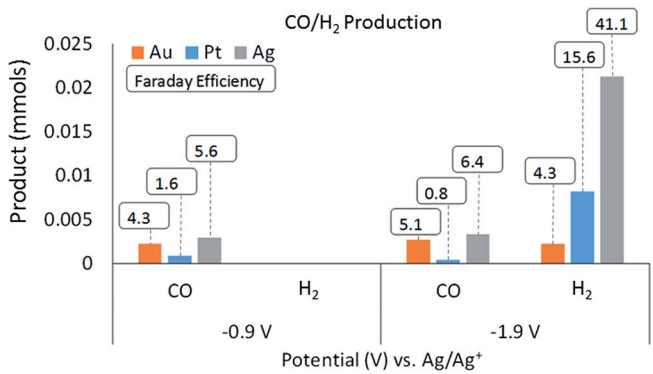

Fig. 4 GC analysis of CO and H_2 production at the Au, Pt, and Ag electrodes after 10 C of charge is passed. Faraday efficiencies (%) for each potential and electrode are shown in the boxes.

using Ag electrodes is displayed in Fig. 3. Electrolysis on Ag resulted in considerably less formate at both −0.9 and −1.9 V, and it should be noted that the maxima for formate production is −0.7 V, at which potential considerably more formate is produced than on the Au electrode.

GC analysis of the headspace gas mixture after electrolysis showed that both CO and H_2 were formed with 0.0022 mmol and 0.0027 mmol of CO produced at −0.9 V and −1.9 V, respectively. This is assigned to the reduction of CO_2 bound to the $[124Triz]^-$ anion (Scheme 4 eqn (3)) and the reduction of CO_2 stabilised by the $[P_{66614}]^+$ cation (Scheme 4 eqn (4)). In addition, hydrogen was only detected at −1.9 V, which is consistent with H_2O being reduced to H_2.

3.2.2 Pt electrode. Quantitative ^1H NMR of the electrolyte after electrolysis showed a similar trend for formate production on Pt compared to Au. A greater quantity of formate was detected at −0.9 V (0.027 mmol) compared with −1.9 V (0.008 mmol) with Faradaic efficiencies of 52.0 and 16.3%, respectively. However, formate production at both potentials was not significantly different from the amount produced using the Au electrode. The OCP prior to electrolysis, but after CO_2 saturation, was more negative than that previously found on Au. It was measured at −0.60 V, giving smaller applied potentials of 0.3 and 1.3 V for electrolysis at −0.9 and −1.9 V, respectively. CO was detected at both −0.9 and −1.9 V, however, the amount of CO detected was significantly reduced at both potentials compared with the analogous reductions over Au and Ag. No H_2 was detected at −0.9 V while significantly more H_2 was detected at −1.9 V on Pt than Au, as expected. This corresponds well with previous reports showing that the order in ability to catalyse the hydrogen evolution reaction is Pt > Au > Ag.[24] This in turn relates to the observed reduction potentials after the addition of H_2O on the Pt, Au and Ag electrodes (−1.5, −1.8 and −1.9 V, respectively). However, more H_2 is detected for Ag electrodes at −1.9 V than over Pt, this is surprising given that Ag has the most negative onset potential for reduction of H_2O to H_2. Previous reports have stated that the IL cation may suppress hydrogen production by blocking H_2O binding. As such, the disparity in hydrogen production may indicate a differing affinity for the cation to the three electrode surfaces, of the order Ag < Pt < Au, as well as the ability of the electrode material to activate water. As such, the production of H_2 and CO may be a balance between catalytic activity (through onset potentials) and binding energy of the reduced species.

Overall, for all three electrodes (Ag, Au and Pt) the trend in the species formed during the reduction is the same, *i.e.* less negative potentials favour formate whereas more negative potentials favour CO and H_2. The main difference between the electrodes is the potential at which the maxima/optimum for each species occur. For example, for formate production, on the Ag electrode this occurs at −0.7 V, which is less negative than found for the Au and Pt electrodes. In addition, it is clear that as the potential becomes more negative the Faradaic efficiency for the species detected decreases for all three electrodes.

4 Conclusions

We have shown that the CO_2 saturated superbasic IL $[P_{66614}][124Triz]$ can be reduced on Au and Pt electrodes to produce formate and syngas. Two reaction pathways appear to exist at −0.9 V and −1.9 V. Formate is formed in increased quantities at −0.9 V over −1.9 V on both electrode surfaces with Faradaic

efficiencies of *ca.* 50% for both electrode surfaces. The production of CO is higher on Au electrodes than Pt electrodes for both electrolysis potentials of −0.9 and −1.9 V. The production of hydrogen, only observed at −1.9 V, is *ca.* 3 times higher on Pt electrodes, enabling the ratio of $CO : H_2$ in the syngas mixture to be influenced by electrode choice. The reduction of physically bound CO_2 is shown to occur at similar potentials on Au electrodes to those reported for ILs that only physically absorb CO_2, such as $[C_4mim][BF_4]$, albeit at lower Faradaic efficiencies.[23] Formate production in ionic liquids has been previously reported to occur on indium surfaces using hydrated CO_2 saturated $[C_2mim][TFA]$.[9] The $[TFA]^-$ anion only very weakly binds to CO_2, which results in little significant activation of the CO_2 and formate production at low Faradaic efficiencies (*ca.* 10%) at 1.55 V *vs.* Ag/Ag^+, rising to 90% efficiency at −1.95 V *vs.* Ag/Ag^+. This behaviour is in good agreement with our proposed onset of reduction of physically bound CO_2. In the present study, the binding of CO_2 is much stronger and, thus, formate production on Au and Pt electrodes, from the chemically bound CO_2, is observed at applied potentials lower than any previously reported ILs. These results show the same trends as found over the previously reported Ag electrode, albeit with some differences. For example, the maximum formate production is found at −0.7 V over Ag at which potential no reduction was observed on Pt and Au.

5 Abbreviations

$[P_{66614}]^+$	Trihexyltetradecylphosphonium
$[C_2mim]^+$	1-Ethyl-3-methylimidazolium
$[C_4mim]^+$	1-Butyl-3-methylimidazolium
$[124Triz]^-$	1,2,4-Triazolide
$[BF_4]^-$	Tetrafluoroborate
$[NTf_2]^-$	Bis(trifluoromethylsulfonyl)imide
$[TFA]^-$	Trifluoroacetate
$[OAc]^-$	Acetate
$[NO_3]^-$	Nitrate

Acknowledgements

This work was carried out as part of the "4CU" programme grant, aimed at sustainable conversion of carbon dioxide into fuels, led by The University of Sheffield and carried out in collaboration with The University of Manchester, Queen's University Belfast and University College London. The authors acknowledge gratefully the Engineering and Physical Sciences Research Council (EPSRC) for supporting this work financially (Grant No. EP/K001329/1). S. F. R. Taylor and N. Hollingsworth wish to thank the ELSOL workshop, Researcher Links, FAPESP and Newton fund for funding. M. T. Galante thanks the RSC and CNPq for funding.

Notes and references

1 S. Solomon, D. Qin, M. Manning, R. B. Alley, T. Berntsen, N. L. Bindoff, Z. Chen, A. Chidthaisong, J. M. Gregory, G. C. Hegerl, M. Heimann, B. Hewitson, B. J. Hoskins, F. Joos, J. Jouzel, V. Kattsov, U. Lohmann,

T. Matsuno, M. Molina, N. Nicholls, J. Overpeck, G. Raga, V. Ramaswamy, J. Ren, M. Rusticucci, R. Somerville, T. F. Stocker, P. Whetton, R. A. Wood and D. Wratt, *Technical Summary, in: Climate Change 2007: The Physical Science Basis. Contribution of Working Group I to the Fourth Assessment Report of the Intergovernmental Panel on Climate Change*, ed. S. Solomon, D. Qin, M. Manning, Z. Chen, M. Marquis, K. B. Averyt, M. Tignor and H. L. Miller, Cambridge University Press, Cambridge, United Kingdom, New York, NY, USA, 2007.

2 T. R. Karl and K. E. Trenberth, *Science*, 2003, **302**, 1719–1723.

3 *Climate Change and Water, Technical Paper of the Intergovernmental Panel on Climate Change*, ed. B. C. Bates, Z. W. Kundzewicz, S. Wu and J. P. Palutikof, IPCC Secretariat, Geneva, 2008, p. 210.

4 P. Styring, E. A. Quadrelli and K. Armstrong, *Carbon Dioxide Utilisation: Closing the Carbon Cycle*, Elsevier Science, 2014.

5 D. T. Whipple and P. J. A. Kenis, *J. Phys. Chem. Lett.*, 2010, **1**, 3451–3458.

6 N. S. Spinner, J. A. Vega and W. E. Mustain, *Catal. Sci. Technol.*, 2012, **2**, 19–28.

7 J. Schneider, H. Jia, J. T. Muckerman and E. Fujita, *Chem. Soc. Rev.*, 2012, **41**, 2036–2051.

8 A. Roldan, N. Hollingsworth, A. Roffey, H. U. Islam, J. B. M. Goodall, C. R. A. Catlow, J. A. Darr, W. Bras, G. Sankar, K. B. Holt, G. Hogarth and N. H. de Leeuw, *Chem. Commun.*, 2015, **51**, 7501–7504.

9 J. D. Watkins and A. B. Bocarsly, *ChemSusChem*, 2014, **7**, 284–290.

10 M. C. Buzzeo, O. V. Klymenko, J. D. Wadhawan, C. Hardacre, K. R. Seddon and R. G. Compton, *J. Phys. Chem. B*, 2004, **108**, 3947–3954.

11 (*a*) L. Sun, G. K. Ramesha, P. V. Kamat and J. F. Brennecke, *Langmuir*, 2014, **30**, 6302–6308; (*b*) J. L. Anthony, J. L. Anderson, E. J. Maginn and J. F. Brennecke, *J. Phys. Chem. B*, 2005, **109**, 6366–6374; (*c*) L. A. Blanchard, D. Hancu, E. J. Beckman and J. F. Brennecke, *Nature (London, U. K.)*, 1999, **399**, 28–29.

12 B. A. Rosen, A. Salehi-Khojin, M. R. Thorson, W. Zhu, D. T. Whipple, P. J. A. Kenis and R. I. Masel, *Science*, 2011, **334**, 643–644.

13 Q. Feng, S. Liu, X. Wang and G. Jin, *Appl. Surf. Sci.*, 2012, **258**, 5005–5009.

14 X. Yuan, B. Lu, J. Liu, X. You, J. Zhao and Q. Cai, *J. Electrochem. Soc.*, 2012, **159**, E183–E186.

15 F. Liu, S. Liu, Q. Feng, S. Zhuang, J. Zhang and P. Bu, *Int. J. Electrochem. Sci.*, 2012, **7**, 4381–4387.

16 B. A. Rosen, J. L. Haan, P. Mukherjee, B. Braunschweig, W. Zhu, A. Salehi-Khojin, D. D. Dlott and R. I. Masel, *J. Phys. Chem. C*, 2012, **116**, 15307–15312.

17 M. Asadi, B. Kumar, A. Behranginia, B. A. Rosen, A. Baskin, N. Repnin, D. Pisasale, P. Phillips, W. Zhu, R. Haasch, R. F. Klie, P. Král, J. Abiade and A. Salehi-Khojin, *Nat. Commun.*, 2014, **5**, 4470.

18 N. Hollingsworth, S. F. R. Taylor, M. T. Galante, J. Jacquemin, C. Longo, K. B. Holt, N. H. de Leeuw and C. Hardacre, *Angew. Chem., Int. Ed.*, 2015, DOI: 10.1002/anie.201507629.

19 (*a*) C. Wang, X. Luo, H. Luo, D.-e. Jiang, H. Li and S. Dai, *Angew. Chem., Int. Ed.*, 2011, **50**, 4918–4922; (*b*) S. Seo, M. A. DeSilva and J. F. Brennecke, *J. Phys. Chem. B*, 2014, **118**, 14870–14879.

20 S. F. R. Taylor, C. McCrellis, C. McStay, J. Jacquemin, C. Hardacre, M. Mercy, R. Bell and N. H. de Leeuw, *J. Solution Chem.*, 2015, **44**, 511–527.

21 L. Aldous, D. S. Silvester, C. Villagran, W. R. Pitner, R. G. Compton, M. Cristina Lagunas and C. Hardacre, *New J. Chem.*, 2006, **30**, 1576–1583.
22 N. S. A. Manan, L. Aldous, Y. Alias, P. Murray, L. J. Yellowlees, M. C. Lagunas and C. Hardacre, *J. Phys. Chem. B*, 2011, **115**, 13873–13879.
23 J. H. Koh, H. S. Jeon, M. S. Jee, E. B. Nursanto, H. Lee, Y. J. Hwang and B. K. Min, *J. Phys. Chem. C*, 2015, **119**, 883–889.
24 F. Zhou, S. Liu, B. Yang, P. Wang, A. S. Alshammari and Y. Deng, *Electrochem. Commun.*, 2014, **46**, 103–106.

